

Far infra-red emission from NGC 7078: First detection of intra-cluster dust in a globular cluster[★]

A. Evans¹, M. Stichel², J. Th. van Loon¹, S. P. S. Eyres³, M. E. L. Hopwood¹, and A. J. Penny⁴

¹ Astrophysics Group, School of Chemistry & Physics, Keele University, Staffordshire ST5 5BG, UK

² Max–Planck–Institut für Astronomie, Königstuhl 17, 69117 Heidelberg, Germany

³ Space Science & Technology Department, CCLRC Rutherford Appleton Laboratory, Chilton, Didcot, Oxfordshire OX11 0QX, UK

⁴ Centre for Astrophysics, University of Central Lancashire, Preston, Lancashire PR1 2HE, UK

Revised 3 July 2003 / Accepted 28 July 2003

Abstract. Improved data analysis of far infrared imaging data of the globular cluster NGC 7078 obtained with the ISO instrument ISOPHOT at 60 μm , 70 μm and 90 μm has detected the thermal emission from dust in its core, the first secure detection of intra-cluster dust in a globular cluster. The amount of dust is broadly consistent with mass-loss from evolved, metal-deficient stars in NGC 7078 in the time since it last crossed the Galactic plane.

Key words. globular clusters: general – infrared: general – globular clusters: individual: NGC 7078 – ISM: general

1. Introduction

As the stars in a globular cluster (GC) evolve and move off the main sequence, they are expected to inject processed material into the intra-cluster environment in the form of gas and dust (Tayler & Wood 1975). However as the GC passes through the plane of the Galaxy, it is scoured clean of this material. Subsequently the intra-cluster environment is replenished by continued stellar mass-loss and will contain an increasing amount of gas and dust, the amount depending on factors such as the number of mass-losing stars, the time since last plane crossing, the escape velocity of the GC etc.

There have been several attempts to detect dust in the cores of GCs at both far infra-red (FIR) and sub-millimetre wavelengths. Gillett et al. (1988) reported a possible detection of dust in the core of NGC 104 with IRAS, although this was not confirmed in subsequent observations with ISO (Hopwood et al. 1999). Lynch & Rossano (1990) carried out a search for emission in the IRAS Point Source and Small Scale Structure Catalogs, and in the IRAS HCON1 Sky Brightness Images, but without success; they suggested that sputtering by the hot halo gas might account for the apparent lack of dust in GCs. Penny et al. (1997) and Hopwood et al. (1998) have searched for dust in GCs at 1200 μm and 850 μm respectively. Penny et al. gave

upper limits only, but Hopwood et al. reported a marginal detection at 850 μm in the core of the metal-rich GC NGC 6356.

Origlia et al. (2002) carried out a deep survey of several GCs with ISOCAM. They concluded that prolific mass-loss occurs primarily near the tip of the red giant branch, is episodic, and does not seem to depend strongly on the GC metallicity.

ISO observations of several GCs were presented by Hopwood et al. (1999); however they reported only upper limits. We present here a re-analysis of the ISO data on the GC NGC 7078 (M 15), which has resulted in a secure detection, and the first detection of intra-cluster dust in a GC.

2. NGC 7078

The relevant properties of NGC 7078 are given by Hopwood et al. (1999). For reference we reproduce and update these here in Table 1, in which the escape velocity V_{esc} is from Webbink (1985), the time T since last plane crossing is from Odenkirchen et al. (1997), the metallicity is from Sneden et al. (1997), the reddening is from Moehler et al. (1995) and the distance is from Durrell & Harris (1993); other data are from compilations in Djorkovski & Meylan (1993).

We re-estimate the expected mass of dust M_{d} in NGC 7078 using (cf. Tayler & Wood 1975)

$$M_{\text{d}} \simeq \frac{T}{\tau_{\text{HB}}} N_{\text{HB}} \frac{\delta M}{100} 10^{[\text{Fe}/\text{H}]}, \quad (1)$$

where τ_{HB} is the Horizontal Branch (HB) lifetime, N_{HB} is the number of HB stars in the cluster, δM is the mass lost by each star at the tip of the red giant branch, and the factor 100 is the gas-to-dust ratio for solar metallicity.

Send offprint requests to: A. Evans,
e-mail: ae@astro.keele.ac.uk

[★] Based on observations with ISO, an ESA project with instruments funded by ESA Member States (especially the PI countries: France, Germany, The Netherlands and the UK) and with the participation of ISAS and NASA.

Table 1. NGC 7078 parameters. See text for details.

[Fe/H]	Core radius r_c	Z-height	T	M_c	V_{esc}	L	$E(B - V)$	D
	($''$)	(kpc)	(years)	(M_\odot)	(km s^{-1})	(L_\odot)		(kpc)
-2.40	4.1	4.79	4×10^7	2×10^6	40.9	5.8×10^5	0.1	10.4 ± 0.8

We take $\tau_{\text{HB}} = 120 \times 10^6$ years (Dorman et al. 1993) and $\delta M = 0.2 M_\odot$ from Tayler & Wood (1975). We estimate N_{HB} for NGC 7078 using the “specific evolutionary flux” B , (Renzini & Buzzoni 1986), which for NGC 7078 is $\sim 2 \times 10^{-11}$ stars $\text{yr}^{-1} L_\odot^{-1}$. Thus $N_{\text{HB}} \simeq BL\tau_{\text{HB}} \simeq 1400$, consistent with the number of HB stars (390) in the HST WFPC2 field observed by Zoccali et al. (2000). The expected dust content of NGC 7078 is therefore $3.7 \times 10^{-3} M_\odot$ (cf. $2.0 \times 10^{-3} M_\odot$ in Hopwood et al. 1999). As the escape velocity for NGC 7078 ($\simeq 40 \text{ km s}^{-1}$) exceeds the typical wind speed for a red giant star ($\lesssim 20 \text{ km s}^{-1}$), we expect that most if not all of the injected material is retained by the GC and likely drops into the core.

3. Observations and data reduction

NGC 7078 was imaged as part of a larger programme of FIR observations of globular clusters (Hopwood et al. 1999) with the photometer ISOPHOT (Lemke et al. 1996; Lemke & Klaas 1999) aboard the Infrared Space Observatory (ISO). The C100 camera (3×3 pixel array, pixel size of $43.''5$) was used to obtain raster maps of NGC 7078 at $60 \mu\text{m}$, $70 \mu\text{m}$ and $90 \mu\text{m}$ at two epochs, 1996 November 1 and 1996 November 26. The raster step sizes for all maps were one full detector size, giving no redundancy between subsequent detector sky positions.

Since the dust emission from NGC 7078 is expected to be weak and highly concentrated, mostly within a single detector pixel, the rejection of cosmic ray hits and the removal of short time-scale detector variations is critical for the detection of faint sources. Because of the non-overlapping raster steps, this is clearly even more important for the maps of NGC 7078. Therefore, the signal for each detector pixel and sky position was derived from the full distribution of pairwise ramp read-out differences rather than from linear fits to the complete read-out ramp, which allow a much larger distribution to be analyzed. This method has been shown to produce significantly deeper images than the standard ramp fitting (Stickel et al. 2003). The derived signals were then corrected for the dependence on ramp integration times to be consistent with calibration observations, dark-current subtracted, and finally flux calibrated with ISOPHOT Interactive Analysis package PIA¹ version 9.1/Cal G version 6.0 (Gabriel et al. 1997). For the conversion of detector signals to fluxes, the average of the signals of the two calibration measurements accompanying each map were used.

After flux calibration, significant differences in the overall sky levels of the pixel data streams were still present,

most likely coming from inappropriately corrected pixel-to-pixel sensitivities (flat field), which moreover appeared to be time-dependent. This would result in severe striping, and checker board patterns in the final maps, reducing significantly the limit for the detection of faint sources. To correct for this, the data streams were smoothed with robust filtering techniques, and each individual data stream rescaled to the common mean, while any residual time trend was removed with robust low-order polynomial fits. A non-linear noise filter (Smith & Brady 1997) and a morphological rolling ball filter (Sternberg 1986) were applied to model the large scale FIR background of the maps, which was subtracted to bring the overall level of the maps within the noise to zero. The $60 \mu\text{m}$, $70 \mu\text{m}$ and $90 \mu\text{m}$ maps were eventually created using the Drizzle mapping method (Hook & Fruchter 1997) within IRAF², where the map pixel size was set to $45.''$; we note that this is well in excess of the core radius r_c of the cluster.

4. Results and discussion

The $60 \mu\text{m}$, $70 \mu\text{m}$ and $90 \mu\text{m}$ maps observed at the first epoch are shown in Fig. 1; the maps from the second epoch are closely similar. A clear signal at the position of the cluster core is seen at all three wavelengths. The flux densities f_ν , in boxes of 3×3 pixels, are given separately for the two epochs in Table 2; they agree within the calibration accuracy of 20–30% and no colour correction has been applied (see below). The mean flux density at each wavelength is also given in Table 2; these fluxes are consistent with the upper limits in Lynch & Rossano (1990) and Hopwood et al. (1999). Similar re-analysis of the ISO data for the other GCs observed by Hopwood et al. (NGC 104, NGC 5319 and NGC 5272) did not lead to any detections, to 3σ limits of 500 mJy ($60 \mu\text{m}$), 600 mJy ($70 \mu\text{m}$) and 300 mJy ($90 \mu\text{m}$).

We determine the stellar contribution to the ISOPHOT fluxes as follows. The surface brightness of NGC 7078 in the UBV bands as a function of distance from the cluster centre has been measured by Newell & O’Neil (1978). For each band we have approximated the intensity distribution by a King (1962)-like function, and numerically integrated the surface brightness out to $67.5.''$, the area over which we have measured the ISOPHOT fluxes. The resultant flux densities, dereddened by $E(B - V) = 0.1$, are included in Fig. 2. The stellar flux measured in 3×3 ISOPHOT pixels will depend on the precise shape of the stellar continuum, which in turn depends on the stellar mix and the spatial distribution of stars close to the core. However

¹ The ISOPHOT data presented in this paper were reduced using PIA, which is a joint development by the ESA Astrophysics Division and the ISOPHOT Consortium. The ISOPHOT Consortium is led by the Max-Planck-Institute für Astronomie, Heidelberg, Germany.

² IRAF is distributed by the National Optical Astronomy Observatories, which are operated by the Association of Universities for Research in Astronomy, Inc., under cooperative agreement with the National Science Foundation.

Table 2. ISOPHOT flux densities. See text for details.

Epoch	$f_v(60\ \mu\text{m})$	$f_v(70\ \mu\text{m})$	$f_v(90\ \mu\text{m})$
	[mJy]		
1996 Nov. 1	460	570	280
1996 Nov. 26	530	690	350
Mean	495	630	315
Colour-correction factors	0.96	1.09	1.04
Colour-corrected fluxes	516	578	303

as the measured ISOPHOT fluxes must lie on the Rayleigh-Jeans tail of the stellar emission, these factors will simply scale the Rayleigh-Jeans tail and the spectral shape of any FIR excess is insensitive to the blackbody temperature taken. We therefore simply approximate the stellar emission by a blackbody at 4200 K (with uncertainty ± 100 K), obtained by fitting a blackbody to the *UBV* photometry; this continuum is also included in Fig. 2.

Inspection of Fig. 2 shows that the FIR spectral energy distribution (SED) of NGC 7078 is clearly inconsistent with the Rayleigh-Jeans tail of emission by its stellar content, the measured FIR emission exceeding the extrapolated stellar continuum by some three orders of magnitude. We also note that the magnitude and wavelength at which the excess is seen means that it is very unlikely to be due to the contribution of circumstellar dust (Origlia et al. 2002). The only plausible explanation for the excess is emission by intra-cluster dust in the GC core.

We quantify the amount of dust in the 3×3 pixels as follows. Assuming that the dust distribution is optically thin, the mass of dust M_d is given by

$$\frac{M_d}{M_\odot} = 4.79 \times 10^{-17} \left(\frac{f_v}{\text{mJy}} \right) \frac{D_{\text{kpc}}^2}{\kappa B(\nu, T_d)}, \quad (2)$$

where D_{kpc} is the distance of NGC 7078 in kpc, κ is the absorption coefficient for the dust (in $\text{cm}^2 \text{g}^{-1}$) and $B(\nu, T_d)$ is the Planck function (in cgs units) at the dust temperature T_d . Detailed calculation by Hopwood (2000) suggests that $T_d \approx 50$ K for silicate dust in NGC 7078 (see also Angeletti et al. 1982). The ISOPHOT colour corrections (Laureijs et al. 2002) for this temperature are listed in Table 2, together with the corresponding colour-corrected flux densities; we use these values in what follows.

The absorption coefficient for a variety of cosmic dust analogues, over the range of temperatures and wavelengths of interest here, have been measured by Mennella et al. (1998). We take here the value for amorphous fayalite at $T_d \approx 50$ K, which varies with wavelength λ as

$$\kappa \approx 0.48 \left(\frac{\lambda(\mu\text{m})}{2000} \right)^{-1.9} \text{ cm}^2 \text{ g}^{-1} \quad (\lambda \gtrsim 30\ \mu\text{m}), \quad (3)$$

obtained by fitting the data in Mennella et al. (1998). For wavelengths $\lesssim 30\ \mu\text{m}$, there is structure in the wavelength-dependence of κ for amorphous fayalite (Mennella et al. 1998), which has no bearing on our discussion and which we ignore here. Although amorphous fayalite is an iron-rich silicate – and therefore unlikely to condense in the winds of GC red giant

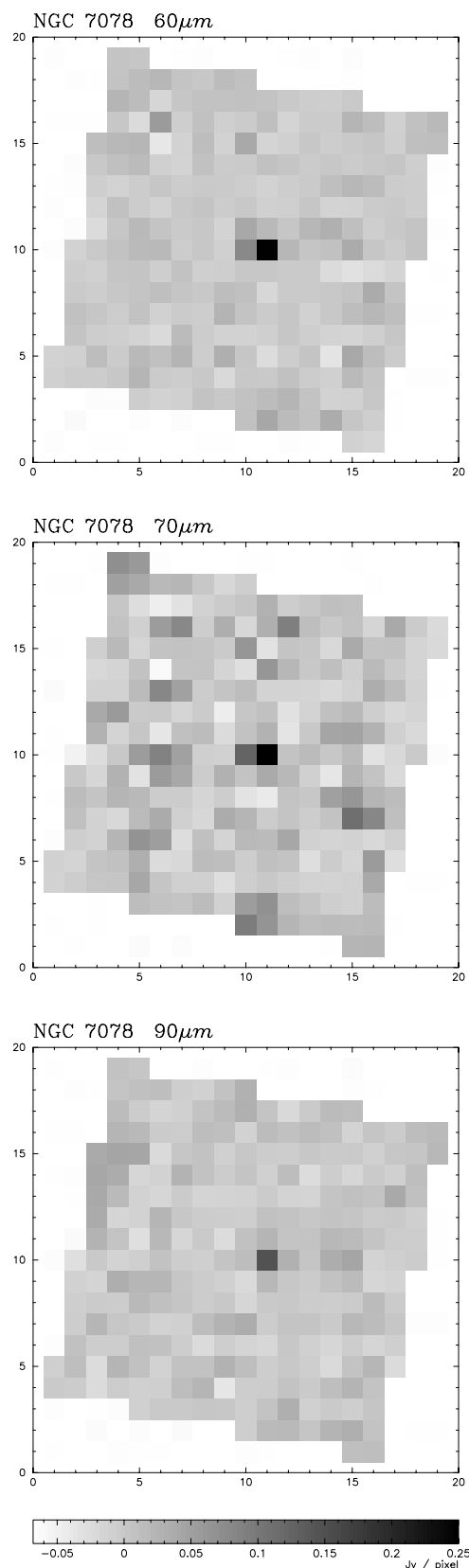


Fig. 1. Gray-scale representation of the ISOPHOT $60\ \mu\text{m}$ (top), $70\ \mu\text{m}$ (middle), $90\ \mu\text{m}$ (bottom) map of NGC 7078 for the first epoch observation; the scale at the bottom applies to all three images. Horizontal and vertical scales are in pixels; pixel size is $45''$.

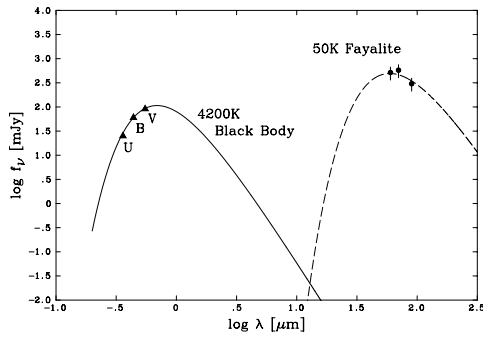


Fig. 2. Colour-corrected ISOPHOT fluxes from central 3×3 pixels of NGC 7078 (filled circles) compared with the stellar contribution (filled triangles). Solid curve is 4200 K blackbody fitted to *UBV* data; broken curve corresponds to fayalite at 50 K. See text for details.

stars – its opacity is typical of a variety of other likely condensates. Indeed for other materials studied by Mennella et al., the values of κ range from an order of magnitude lower, to an order of magnitude larger, than that for amorphous fayalite.

We have fitted a function of the form $\lambda^{-1.9} B(\nu, T_d)$ to the FIR excess; the fit is included in Fig. 2. The implied dust mass, which scales in proportion to grain size, is $4.8(\pm 1.6) \times 10^{-4} M_\odot$ for $0.1 \mu\text{m}$ grains. Note that this result is a factor ~ 10 lower than the 3σ upper limits on dust mass in Hopwood et al. (1999). The uncertainty in the dust mass includes the uncertainty in the ISOPHOT calibration and in the placement of the stellar continuum. It does not include uncertainties in κ arising from uncertainty in the dust composition, T_d and grain size; allowing for these renders the dust mass uncertain to a factor ± 1 dex (see above and Mennella et al. 1998).

Nonetheless it is gratifying to see that the observed dust mass is within an order of magnitude of the prediction of Eq. (1) and that, given the above uncertainties, the dust content of the core of NGC 7078 is reasonably in line with its metallicity, its HB star content and the time since its last plane crossing.

5. Conclusions

We have reported the detection of a significant FIR excess in the SED of NGC 7078, the first unambiguous detection of emission by intra-cluster dust in any GC. Within the uncertainties, the corresponding dust mass is consistent with the expected HB star content of NGC 7078 and their mass-loss, after allowing for their metal-deficiency.

Our results demonstrate that the routine detection of dust in the cores of GCs is now tantalizingly close, and will surely be within the reach of forthcoming FIR observatories such as SIRTF. Further FIR observations of GCs with these facilities must be a priority to increase the number of known GCs with dust, and to understand the mechanism of dust formation and stripping in metal-rich and metal-deficient GCs.

Also, the expected flux density at $450 \mu\text{m}$ ($850 \mu\text{m}$) is ~ 3 mJy (~ 0.3 mJy), and may be within the capability of the next generation of sub-millimeter continuum instruments such as SCUBA2 (Holland et al. 2003). Further studies of GCs at these wavelengths is also merited.

Acknowledgements. The development and operation of ISOPHOT were supported by MPIA and funds from Deutsches Zentrum für Luft- und Raumfahrt (DLR, formerly DARA). The ISOPHOT Data Centre at MPIA is supported by DLR with funds of Bundesministerium für Bildung und Forschung, grant No. 50 QI0201.

References

- Angeletti, L., Capuzzo-Dolcetta, R., Giannone, P., Blanco, A., & Bussoletti, E. 1982, *MNRAS*, 199, 411
- Djorkovski, S. G., & Meylan, G. (eds.) 1993, *Structure and Dynamics of Globular Clusters*, ASP Conf. Ser., 50
- Dorman, B., Rood, R. T., & O’Connell, R. W. 1993, *ApJ*, 419, 596
- Durrell, P. R., & Harris, W. E. 1993, *AJ*, 105, 1420
- Gabriel, C., Acosta-Pulido, J., Heinrichsen, I., et al. 1997, *Astronomical Data Analysis Software and Systems VI*, ed. G. Hunt, & H. E. Payne, ASP Conf. Ser., 125, 108
- Gillett, F. C., de Jong, T., Neugebauer, G., Rice, W. L., & Emerson, J. P. 1988, *AJ*, 96, 116
- Holland, W. S., Duncan, W., Kelly, B. D., et al. 2003, *SPIE*, 4855, 1
- Hook, R. N., & Fruchter, A. S. 1997, *Astronomical Data Analysis Software and Systems VI*, ed. G. Hunt, & H. E. Payne, ASP Conf. Ser., 125, 147
- Hopwood, M. E. L., 2000, Ph.D. Thesis, Keele University
- Hopwood, M. E. L., Evans, A., Penny, A., & Eyres, S. P. S. 1998, *MNRAS*, 301, L30
- Hopwood, M. E. L., Eyres, S. P. S., Evans, A., Penny, A., & Odenkirchen, M. 1999, *A&A*, 350, 49
- King, I. R. 1962, *AJ*, 67, 471
- Laureijs, R. J., Klaas, U., Richards, P. J., Schulz, B., & Ábrahám P., 2002, *The ISOPHOT Handbook*, http://www.iso.vilspa.esa.es/manuals/HANDBOOK/pht_hb/
- Lemke, D., Abolins, J., Abraham, P., et al. 1996, *A&A*, 315, L64
- Lemke, D., & Klaas, U. 1999, in *The Universe as seen by ISO*, ed. P. Cox, & M.F. Kessler, ESA-SP 427, 55
- Lynch, D. K., & Rossano, G. S. 1990, *AJ*, 100, 719
- Mennella, V., Brucato, J. R., Colangeli, L., et al. 1998, *ApJ*, 496, 1058
- Moehler, S., Heber, U., & de Boer, K. S. 1995, *A&A*, 294, 65
- Newell, B., & O’Neil, E. J. 1978, *ApJS*, 37, 27
- Odenkirchen, M., Brosche, P., Geffert, M., & Tucholke, H.-J. 1997, *New Astron.*, 2, 477
- Origlia L., Ferraro F. R., Fusi Pecci F., Rood R. T., 2002, *ApJ*, 571, 458
- Penny, A. J., Evans, A., & Odenkirchen, M. 1997, *A&A*, 317, 694
- Renzini, A., & Buzzoni, A. 1986, in *Spectral evolution of galaxies*, ed. C. Chiosi, A. Renzini, & D. Reidel (Dordrecht), 195
- Smith, S. M., & Brady, J. M. 1997, *Int. J. Comp. Vis.*, 23, 45
- Snedden, C., Kraft, R. P., Shetrone, M. D., et al. 1997, *AJ*, 114, 1964
- Sternberg, S. 1986, *Comp. Vis. Graph. Image Proc.*, 35, 333
- Stickel, M., Bregman, J. N., Fabian, A. C., White, D. A., & Elmegreen, D. M. 2003, *A&A*, 397, 503
- Taylor, R. J., & Wood, P. R. 1975, *MNRAS*, 171, 467
- Webbink R.F., 1985, in *Proc. IAU Symp. 113*, ed. J. Goodman (Dordrecht: Reidel), 541
- Zoccali, M., Cassisi, S., Bono G., et al. 2000, *ApJ*, 538, 289